

**The role of the Amazon Basin moisture in the atmospheric branch of the
hydrological cycle: A Lagrangian analysis**

Anita Drumond ^{1 *}, Jose Marengo ², Tercio Ambrizzi ³, Raquel Nieto ¹, Lorena
Moreira ⁴, Luis Gimeno ¹

1 Ephyslab, Facultad de Ciencias, UVIGO, Ourense, Spain.

2 CCST INPE, Cachoeira Paulista, Sao Paulo, Brazil

3 Instituto de Astronomia, Geofisica e Ciencias Atmosfericas, USP, Sao Paulo, Brazil

4 Institute of Applied Physics, University of Bern, Bern, Switzerland

(*) Corresponding author: Anita Drumond. Departamento de Física Aplicada, Facultad
de Ciencias de Ourense, Universidad de Vigo, Campus As Lagoas s/n, Ourense,
Spain, 32004. e-mail: anitadru@uvigo.es fax: 34988387227

(submitted to Hydrology and Earth System Sciences in December 2013)

(2nd version submitted to Hydrology and Earth System Sciences in April 2014)

(3rd version submitted to Hydrology and Earth System Sciences in May 2014)

The role of the Amazon Basin moisture in the atmospheric branch of the hydrological cycle: A Lagrangian analysis

Abstract

We used a Lagrangian model (FLEXPART) together with the 1979-2012 ERA Interim reanalysis data to investigate the role of the moisture in the Amazon Basin in the regional hydrological budget over the course of the year. FLEXPART computes budgets of evaporation minus precipitation by calculating changes in the specific humidity along forward and backward trajectories. The Tropical Atlantic is the most important remote moisture source for the Amazon Basin. The Northern Tropical Atlantic (NA) mainly contributed during the austral summer, while the contribution of the Southern Tropical Atlantic (SA) prevailed for the remainder of the year. At the same time, the moisture contribution from the Amazon Basin itself is mainly for moisture supplying the southeastern South America. The 33-year temporal domain allowed the investigation of some aspects of the interannual variability of the moisture transport over the basin, such as the role of the El Niño Southern Oscillation (ENSO) and the Atlantic Meridional Mode (AMM) on the hydrological budget. During the peak of the Amazonian rainy season (from February to May, FMAM) the AMM is associated more with the interannual variations in the contribution from the tropical Atlantic sources, while the transport from the basin towards the subtropics responds more to the ENSO variability. The moisture contribution prevailed from the SA (NA) region in the years dominated by El Niño/AMM+ (La Niña/AMM-) conditions. The transport from the Amazon towards the subtropics increased (reduced) during El Niño (La Niña) years.

Keywords: Moisture transport, Amazon basin, Lagrangian scheme

1. Introduction

The Amazon basin contains a great variety of ecosystems, including the largest tropical forest on the planet. Precipitation is approximately 2,300 mm/year and the discharge of the Amazon River into the Atlantic Ocean corresponds to 18% of the total discharge of freshwater into the oceans. This river drains an area of $6.2 \times 10^6 \text{ km}^2$ and discharges an average of 6300 km^3 of water to the Atlantic Ocean annually (Marengo and Nobre, 2009). It is known that the Amazon rainforest plays an important role in the global energy and hydrological budgets, and has been suffering for some time from intense deforestation. Unfortunately, the temporal and spatial data coverage is poor over the basin and most studies are based on numerical products (reanalysis projects) and observational data over just a few points for a short period of time.

The climatological annual cycle of precipitation is not homogeneous over the Amazon, and the start and end of the rainy season vary gradually from the southern basin northwards (e.g., Marengo et al., 2001; Liebmann and Marengo, 2001; Carvalho et al., 2011). In the southern part of the basin the rainy season occurs between austral Spring and Autumn, while over the western and the northern Amazon it extends from austral Autumn to Spring.

The role of Amazonian forest in the hydrological cycle of the region has received a fair amount of attention in recent decades. The ratio of the amount of precipitation that comes from a local region through evaporation to the total observed is known as the “recycling” ratio, and has been the subject of study since the mid-1970’s (see Molion [1975] and Salati et al [1987] and the references quoted therein). This ratio varies

substantially, assuming a generally lower value in winter and a generally higher value in summer, when large-scale transport diminishes in importance. Precipitation recycling is the contribution of evaporation from within a region to precipitation in that same region. The recycling rate is a diagnostic measure of the potential interaction between land surface hydrology and regional climate. The recycling of local evaporation and precipitation by the forest accounts for a sizable portion of the regional water budget, and because large areas of the basin are sensitive to the effects of deforestation there are grave concerns about how such disruptions to the land surface may affect the hydrological cycle in the tropics. Eltahir and Bras (1994), Brubaker et al., (1993), Costa and Foley (1999), Trenberth (1999), Nobrega et al (2005), Marengo et al (2006), Silva (2009), Van der Ent et al. (2010), and Satyamurty et al (2013), among others have estimated an annual mean recycling rate of about 20% to 35%, less than the previous estimates made by Molion. Dirmeyer et al (2009) combines the characteristics of persistence of soil moisture anomalies, strong soil moisture regulation of evaporation rates, and reinforcement of water cycle anomalies through recycling, and they demonstrated that there are signs of land–atmosphere feedback throughout most of the year in the Amazon region. More recently, in their study of the role of land surface processes and land use changes in regional circulation, Angelini et al. (2011) found that rain in Amazonia comes primarily from large-scale weather systems from the tropical Atlantic that do not rely on local evaporation. Previous studies by Gat and Matsui (1991) and references quoted therein investigate the moisture recycling in the Amazon region using the isotopic composition of precipitation over the region. Their results suggest that an isotopically fractionated evapotranspiration flux contributes to the atmospheric water balance over the region, and they show that 20–40% of the total

1 evapotranspiration flux is accompanied by an isotopic fractionation, such as by
2 evaporation from an open water surface.

3
4 Almost all the studies concerning moisture transport over the Amazon are based on
5 Eulerian methodologies (e.g., Arraut and Satyamurty, 2009; Arraut et al., 2012;
6 Satyamurty et al., 2013 and references quoted therein). According to these authors, the
7 moisture flux from the equatorial Atlantic associated with the trade winds is the main
8 remote moisture source for the Amazon. The climatological role of the Atlantic
9 subtropical ocean as a moisture source for the Amazon was also reported in the
10 Lagrangian 5-yr periodic analysis developed by Stohl and James (2005), as well as in
11 the recent results on the role of the oceanic regions published by Gimeno et al. (2013).
12 At the same time, the air mass trajectories crossing the Amazon capture moisture
13 destined for other parts of the continent, particularly the La Plata Basin and Central
14 Brazil (e.g., Roads et al., 2002; Marengo, 2005; Drumond et al., 2008; Arraut and
15 Satyamurty, 2009). Van der Ent et al. (2010) verified that the La Plata basin relies on
16 evaporation from the Amazon forest for 70% of its water resources. Bosilovich et al
17 (2006) suggested that evaporation from the Amazon River basin exhibits slight
18 interannual variations, and in turn the interannual variation of precipitation recycling is
19 therefore related to atmospheric moisture transport from the tropical South Atlantic
20 Ocean.

21
22 The role of vegetation in supplying moisture transport over the Amazon was discussed
23 by Spracklen et al. (2012), who found that air that passes over extensive vegetation
24 subsequently releases at least twice as much rain a few days later than air that passes
25 over less vegetated areas. More recently, Makarieva et al. (2013) suggested that the

1 water vapour delivered to the atmosphere via evaporation from forests represents a store
2 of potential energy available to accelerate air and drive winds. This implies that changes
3 in precipitation over Amazonia are due to a combination of different regional processes
4 and interactions that are partly influenced by large-scale circulation and partly
5 influenced by local water sources from forests and soil moisture.

6
7 Several of the drought episodes documented in the Amazon occurred during intense El
8 Niño episodes, such as those registered in 1926, 1983, 1997-98, and 2010, with
9 reductions in discharge in the main rivers as well as serious ecological and economical
10 damage due to fire events (e.g., Williams et al. 2005; Sternberg, 1987; Marengo et al.
11 2008, 2013; Richey et al., 1989). The influence of the El Niño Southern Oscillation
12 (ENSO) in the interannual variability of the Amazon climate may also be felt due to its
13 role in positioning the Inter Tropical Convergence Zone (ITCZ) (e.g., Coe et al., 2002;
14 Uvo et al., 1998, Marengo et al., 2013). Although the impact of the ENSO on the
15 Amazon precipitation and river discharge has been investigated extensively, its
16 influence on the moisture transport into and out of the basin has not been explored in
17 any detail. It is known that during ENSO events, changes in precipitation regime are
18 greater during the Amazon rainy season, and they are not homogeneous over the basin
19 (Foley et al., 2002, Marengo et al., 2008). As mentioned by Grimm and Ambrizzi
20 (2009, and references quoted therein), during El Niño episodes the tropical convection
21 is shifted from western Pacific towards central and east Pacific. Consequently, the
22 Pacific Walker cell is weakened, because the induced anomalous circulation along the
23 equator is opposite to the climatological circulation. As the anomalous subsidence in the
24 Walker cell associated with anomalous convection over the eastern Pacific occurs over
25 northern South America and Atlantic Ocean, the two smaller cells connected with the

continent are strongly affected, especially by the weakening of the ascending branch over the Amazon region. The reduction of the convection over this region also reduces the regional Hadley circulation. On the other hand, the Hadley circulation is strengthened over the central/eastern Pacific. During La Niña episodes the changes are nearly opposite.

Nevertheless, not all El Nino events are related to drought in the Amazon (Marengo et al., 2013). Recent studies have also pointed to the importance of the tropical Atlantic (TA) in the modulation of the Amazon climate (Yoon and Zeng, 2010), as observed during the 2005 and 2010 drought events (e.g., Marengo et al., 2008; Lewis et al., 2013), as well as during the 2012 flood in the Amazon River (Satyamurty et al., 2013). According to Servain (1991), the Atlantic Meridional Mode (AMM), also known as the meridional SST gradient, may be considered one of the main low frequency SST variability modes in the Tropical Atlantic, and its extreme episodes are characterised by an anomalous interhemispheric gradient structure. Associated with these anomalous SST patterns are changes in the trade winds, presenting as anomalous surface winds crossing equator, and the Atlantic ITCZ is displaced towards the warmer SST anomalies.

Given the importance of the Amazon basin in the moisture budget, the present paper aims to investigate the annual cycle of the main sources of moisture for the Amazon basin, as well as its own contribution as a moisture source for the rest of the continent, through the use of the Lagrangian method developed by Stohl and James (2004, 2005). This approach diagnoses net changes in specific moisture along trajectories and was previously successfully applied in studies of sources of moisture for different regions

around the world, including South America, such as the Orinoco River basin (Nieto et al., 2008), the South American Monsoon System (SAMS), and Northeastern Brazil (Drumond et al., 2008, 2010). Here we make use of a 33-year data set that allows us to corroborate the climatological aspects highlighted by the 5-year analysis of Stohl and James (2005), and to explore aspects of interannual variability in a novel way. The larger temporal domain allows the investigation of the changes observed during years characterised by extreme conditions of the ENSO and of the AMM on the moisture transport over the region.

2. Data and Methods

The Amazon basin is shown in Figure 1. The spatial limits adopted for this domain are in accordance to those defined by the Observatoire de Recherche en Environnement (ORE HYBAM) in the website <http://www.ore-hybam.org/index.php/por/Dados/Cartografia/Bacia-amazonica-hidrografia>.

A detailed intercomparison of the different methods used to establish source-sink relationships for atmospheric water vapor is given by Gimeno et al. (2012). There are different methods, namely “analytical and box models”, “physical water vapor tracers” (isotopes), and “numerical water vapor tracers” (including the Lagrangian and Eulerian approaches). All of them provide useful and interesting information that aids the analysis and the results are subject to assumptions made and to the type and accuracy of the data used. The “box models” allow the identification of the moisture inflow and outflow given defined lateral boundaries, but they give no information about the physical processes that occur within the box itself. The use of isotopes depends on

1 the sensitivity of the isotopic signal. The Eulerian methodology is widely used due its
2 simplicity but it is not simple to extract the link between the precipitation over a region
3 and the moisture source using this method. The Lagrangian approach provides realistic
4 traces of air parcels, enabling the trajectories to be followed and source-receptor
5 relationships to be established. In that way, the most recently developed Lagrangian
6 techniques are being extensively applied for evaluating the origin of the water that
7 precipitates over a continental area (e.g., Stohl and James, 2005; Dirmeyer and
8 Brubaker, 2007; Gimeno et al., 2013; Knippertz et al., 2013).

9
10 The present study is based on the method developed by Stohl and James (2004, 2005),
11 which uses the FLEXPART V9.0 Lagrangian particle dispersion model and ERA-
12 Interim Reanalysis data (Dee et al., 2011) to track changes in atmospheric moisture
13 along trajectories. The model run considers the atmosphere to be divided
14 homogeneously into three-dimensional finite elements (hereafter ‘particles’), each
15 representing a fraction of the total atmospheric mass (Stohl and James, 2004). These
16 particles are advected using the three-dimensional wind data, with superimposed
17 stochastic turbulent and convective motions. The increases (e) and decreases (p) in
18 moisture along any trajectory can be calculated through changes in (q) with time ($e-p =$
19 $m dq/dt$), with (m) being the mass of the particle. By summing ($e-p$) for all the particles
20 residing in the atmospheric column over an area we obtain the aggregated ($E-P$) field,
21 where the surface freshwater flux (E) is the evaporation rate and (P) is the precipitation
22 rate per unit area. It should be noted that this approach has the disadvantage that it
23 cannot calculate evaporation and precipitation separately, but only the fluxes into or out
24 of the tracked air mass. The method is mostly limited by the accuracy of the trajectories
25 and also by the use of a time derivative of humidity (unrealistic fluctuations in humidity

could be considered moisture fluxes). However, such random errors may cancel each other out given the large number of particles in an atmospheric column. A detailed review of this methodology against other Eulerian and Lagrangian approaches was presented by Gimeno et al. (2012).

The FLEXPART data set used in this work comes from a global simulation in which the entire global atmosphere was divided into approximately 2.0 million particles. Following the seminal works of Stohl and James (2004, 2005) and the subsequent studies based on the same lagrangian methodology (e.g., Nieto et al., 2008, Drumond et al., 2008, Gimeno et al., 2013), we limited the transport time to 10 days. While the 10-day period of tracking is somewhat arbitrary, it is about the average residence time of water vapour in the atmosphere (Numaguti, 1999). The tracks were computed using ERA-Interim Re-analysis data available at six-hour intervals (00, 06, 12 and 18 UTC), at a 1° horizontal resolution, and at a vertical resolution including 61 vertical levels, from 0.1 to 1000 hPa. The analysis covers a 33-year period, from June 1979 to May 2012. As Gimeno et al. (2013) pointed out, the FLEXPART model requires consistent high-quality wind and humidity data, meaning that its application to previous years is rather difficult (i.e., prior to the significant decrease in the errors in these variables, particularly over the oceans, due to the inclusion of satellite data in about 1979 (Bengtsson et al., 2004)).

The first question we intend to explore through a Lagrangian analysis is: Where does the atmospheric moisture observed over the Amazon come from? To answer this, a *backward* analysis allows us to identify where the particles gain humidity along their trajectories towards the target area, regions hereafter denominated as sources of

1 moisture. From this set of experiments, in all grid points where $E-P > 0$ we know that
2 air particles located within that vertical column and bound towards the target area gain
3 moisture. A complementary question would be: What is the final destination of the
4 moisture carried by moisture transport along air trajectories leaving the Amazon? In this
5 case, a *forward* analysis may identify all trajectories crossing the basin, and if we follow
6 them we will find where they lose moisture. In this case, the ($E-P < 0$) values indicate
7 the most important sinks of moisture, i.e., where the atmospheric moisture budget of the
8 tracked air particles is characterised by a loss of moisture. All figures show $E-P$
9 integrated over the whole tracking period (10 days) at the monthly scale, allowing us to
10 study the annual cycle. It is important to clarify that the applied methodology does not
11 guarantee that the moisture gained by an air particle when crossing a source will reach
12 the target region. This depends on the interaction with all air particles present in the
13 atmospheric column. In addition, the water may precipitate if the air particle crosses a
14 sink region before reaching the target. Herein we refer to the austral seasons (summer is
15 from December to February, Autumn from March to May, Winter from June to August,
16 and Spring from September to November).

17
18 Given our climatological overview of the atmospheric branch of the hydrological cycle
19 over the Amazon region, our next question is: Were there changes in the moisture
20 transport over the Amazon during years characterised by extremes of ENSO? This
21 theme will be explored through the technique of composite differences. The ENSO
22 events were obtained from the NOAA/CPC Oceanic Niño Index (ONI)
23 (www.cpc.noaa.gov/products/analysis_monitoring/ensostuff/ensoyears.shtml). The
24 index values were calculated as the 3-month running mean of ERSST.v3b SST
25 anomalies (Smith et al. 2008) in the Niño 3.4 region ($5^{\circ}\text{N} - 5^{\circ}\text{S}$, $120^{\circ}\text{W} - 170^{\circ}\text{W}$)

referred to by Trenberth (1997), and the ONI is based on the 1981-2010 climatology. According to CPC, extreme ENSO episodes occur when the threshold of $\pm 0.5^{\circ}\text{C}$ for the ONI is exceeded on a minimum of five consecutive overlapping seasons. Therefore, in order to select a whole year as El Niño or La Niña, we considered those years when the threshold was exceeded a minimum of five times consecutively from June in year 0 to May in year 1 (for a given ENSO cycle). Ten El Niño episodes (1982/83, 1986/87, 1987/88, 1991/92, 1994/95, 1997/98, 2002/03, 2004/05, 2006/07, 2009/10) and eleven La Niña events (1984/85, 1988/89, 1995/96, 1998/99, 1999/00, 2000/01, 2005/06, 2007/08, 2008/09, 2010/11, 2011/12) were selected for the period 1979 – 2012. Although the February-May (FMAM) season was defined to be the peak season for rainfall anomalies in the Amazon (Marengo et al., 2013b), the analysis was carried out at a monthly scale considering the annual cycle from June in one year to May in the following year (June/0 to May/1). This allows us to identify possible changes in moisture transport during the months before the peak season, and also to standardise the presentation of the results according to the ENSO cycle. We followed the methodology proposed by Wei et al. (2012) to evaluate the statistical significance of the composite differences using the Bootstrap method, applied in our case with 1,000 interactions at the 90% confidence level. We repeated the calculation of the difference of two samples (one with 10 elements, and the other with 11) selected at random (a total of 21 elements) from the 33-yr climatology a total of 1,000 times. To be considered significant, the absolute value of the composite of the differences had to be larger than 90% of the 1,000 randomly obtained differences.

Finally, the technique of composite differences was also applied to investigate the influence of the AMM over the moisture transport into and out of the Amazon. We

calculated the AMM index following the method applied by Marengo et al. (2013), using the HadISST1 monthly SST data set (Rayner et al., 2003) available at a 1° regular horizontal resolution to calculate the difference in the standardised SST anomalies averaged over the tropical North Atlantic (12°N-27°N, 20°W-50°W) and the tropical South Atlantic (0°-15°S, 0°W-15°W) subregions. Those years with absolute AMM values averaged over FMAM higher than one standard deviation were considered extremes. AMM+ episodes are herein defined as those presenting positive SST anomalies over the North Atlantic and negative ones over the South Atlantic. The opposite pattern occurs during AMM- events. Applying the same calendar used to study the impacts of the ENSO, the differences in the composites were calculated on a monthly scale considering the annual cycle from June in year 0 to May in year 1. Considering the months FMAM to belong to year 1, seven AMM+ episodes (1979/80, 1980/81, 1982/83, 1991/92, 1996/97, 2003/04, 2009/10) and seven AMM- events (1983/84, 1984/85, 1985/86, 1988/89, 1993/94, 1994/95, 2008/09) were selected from the period 1979 – 2012. To evaluate the statistical significance of the composite differences using the Bootstrap method, the calculation of the difference considered two samples with 7 elements, each selected at random (a total of 14 elements) from the 33-year climatology.

Summarizing, the results presented in the next section are organized into three topics. An analysis of the climatological annual cycle of the transport of moisture into and from the Amazon is discussed in the section 3.1. The technique of composite differences is then applied to investigate how ENSO (section 3.2) and AMM (section 3.3) episodes may affect the transport of moisture over the basin.

3. Results

3.1 Annual Cycle

Figure 1 shows the monthly values of 10-day integrated atmospheric moisture budget ($E-P$) obtained via backward trajectories from the Amazon Basin for the 33-year period June 1979– May 2012. The backward experiment allows us to identify where the tracked particles gain humidity along their trajectories towards the target area. The areas characterised by reddish colours represent regions where $(E-P) > 0$, meaning that evaporation exceeds precipitation in the net moisture budget considering only those air particles located within that vertical column and travelling towards the target area, and these regions act as moisture sources for the tracked particles. In the opposite sense, the blueish colours represent areas where $(E-P) < 0$, which are those regions where precipitation exceeds evaporation in the net moisture budget of the tracked air particles (moisture sinks). Finally, the white areas represent regions where $(E-P)$ values are low.

We now describe the temporal evolution of the distribution of the moisture sources for the Amazon basin throughout the year. The Era-Interim vertically integrated moisture flux (VIMF) and its divergence fields were provided together with the lagrangian backward analyses in order to help the reader to visualize the moisture transport under an Eulerian perspective. Although not shown together, the VIMF fields presented with the backward figures may be useful to interpret the forward analyses as well. The reddish colours configured during the period June-August in Figure 1 suggest the predominance of the contribution from the southern Atlantic ocean, compared with those from northeastern Brazil, the southern Amazon, and the La Plata Basin. It seems that tropical and subtropical South America provide some moisture during the austral

1 winter. Apart from the La Plata basin, the evaporative sources described above coincide
2 quite well with the areas of divergence of the vertically integrated moisture flux (herein
3 VIMF; right-hand column). One can identify some predominantly evaporative sources
4 over the Northern Atlantic (yellow colours, left-hand column), but our methodology
5 cannot be used to check whether the moisture received by the particles crossing this
6 region will precipitate when crossing the ITCZ (blueish equatorial areas) before
7 reaching their target. From September onwards, the moisture sink areas (left-hand
8 column) and the convergence of the VIMF observed over the northwestern Amazon
9 expand towards southeastern Brazil and the La Plata Basin, and persist until March. The
10 persistence of these moisture sink regions through the extended austral summer
11 coincides with the active phase of the SAMS. From November to April, the evaporative
12 sources and the divergence of the VIMF intensify over the tropical North Atlantic ocean
13 and reach the northern boundary of the basin, accompanied by a moisture flux from the
14 northern hemisphere towards the target region. The displacement northwards of the
15 equatorial sink during May is accompanied by a weakening of this evaporative region.

16
17 From the foregoing, Figure 1 suggests the role of the TA as the most important remote
18 source of moisture for the Amazon Basin, probably associated with the seasonal
19 migration of the ITCZ and the confluence of trade winds. It seems that there is an
20 increase in the moisture contribution from the Northern or Southern TA during the
21 respective winter associated with the intensification of the hemispheric trade winds.
22 Nieto et al. (2008) also reported a similar annual cycle in the role of TA as a source of
23 moisture for the Orinoco basin, to the north of the Amazon. Some moisture from the
24 South American Pacific coast also reaches the Amazon throughout the year. The
25 Amazon receives some moisture from subtropical South America, probably transported

by frontal systems. Figure 1 also suggests the contribution of local evaporative processes in the Amazon as a moisture source for the basin throughout the year.

To illustrate the annual cycle of the contribution of the TA in more detail, we divided the region into two hemispheric subareas having the same spatial dimensions: the Northern and the Southern TA (NA: 55°W - 35°W and 2°N - 12°N; SA: 37°W - 17°W and 4°S - 14°S), as indicated in Fig. 2a. The technique of percentiles was applied to the annual averages of (E-P) for both the backward and the forward experiments (Figures 2a and 4a, respectively), in order to determine the boundaries of the areas of interest. Although the definition of the threshold was arbitrary, we believe that this statistical procedure is valid for identifying the regions of maximum absolute (E-P) values. To provide a standardised analysis, we chose the contour line of 0.4 mm/day, which corresponds to the 96% percentile of all positive values shown in Figure 2a, as well as to the 95% percentile of all negative values configured in the (E-P) annual average from the forward experiment (Figure 4a), which we discuss later. The location of the NA and SA boxes coincide with two regions of high values of continental evaporation cycling ratio ($E_c > 0.5$) identified by Van der Ent and Savenije (2013), which represents the fraction of the evaporation that is transported to and precipitates in continents.

Figure 2b shows the monthly averages of the 10-day (E-P) backward trajectories calculated in Figure 1 and integrated over both source areas. Recalling that we define a region as a moisture source when it presents positive (E-P) values, it seems that the NA (continuous black line) contributes moisture from October to May. During this period, the convergence of VIMF associated with the ITCZ migrates southwards, and the northern trade winds carrying moisture cross the NA and reach the southern American

coast (Figure 1, right-hand column). The negative ($E-P$) values characterising the NA from June to September suggest that this region does not act as a moisture source for the Amazon basin during these months. In our methodology, this means that precipitation prevails over evaporation in the atmospheric moisture budget integrated over NA during this period. This may be the case because the positioning of the VIMF convergence associated with the Atlantic ITCZ in these months (Figure 1, right-hand column) coincides with the NA box. On the other hand, the contribution of the SA (traced black line) occurs all year and reaches its maximum during the austral winter, when the VIMF divergence over the South Atlantic is greater and expands into the tropical continent, enhancing the moisture flux towards the Amazon (Figure 1, right-hand column). Our results compare well with those of Bosilovich and Chern (2006) and of Van der Ent and Savenije (2013). Bosilovich and Chern (2006) made use of a 50-year atmospheric general circulation model simulation including water vapour tracers to investigate the water budget for the Amazon River and its respective sources of water. These authors also noted the importance of the South Atlantic ocean in providing moisture to the Amazon Basin throughout the year, except during the austral summer when the contribution of the tropical North Atlantic dominates. Using a different methodology from that applied in the present study to identify the oceanic sources based on an atmospheric backtracking analysis of continental precipitation, Van der Ent and Savenije (2013) also verified not only the importance of the TA in providing moisture to South American precipitation, but also a similar variability of the contributions from the northern and southern TA throughout the year.

The role of the Amazon as a moisture source can be inferred from the 10-day ($E-P$) forward trajectories from the basin for the 33-year period presented in Figure 3. The

1 method identifies those particles that leave the basin and follows them to the point at
2 which they lose moisture. Only negative values are shown in order to clarify the
3 moisture sinks. The white areas represent regions where the ($E-P$) fields have low or
4 positive values. We will now briefly describe the temporal evolution. During the austral
5 winter months the major moisture sinks of the air particles that leave the basin are
6 located over southeastern South America and over northern South America and adjacent
7 equatorial regions. These sinks coincide with two regions of convergence of VIMF over
8 the continent: one over the subtropics, and another associated with the ITCZ (Figure 1,
9 right-hand column). From September to January, the moisture transport towards the
10 equatorial latitudes weakens in association with the weakening of the convergence of
11 the VIMF (Figure 1, right-hand column), while the moisture sinks and the convergence
12 of the VIMF areas expand over tropical and subtropical South America. During the
13 austral autumn, the convergence of the VIMF and the sink regions reduce again towards
14 both the subtropics of the continent and the equatorial band.

15
16 In accordance with the VIMF analysis shown in Figure 1 (right-hand column) and in
17 view of previous results obtained using different methodologies (e.g., Roads et al. 2002;
18 Marengo, 2005, 2006; Drumond et al., 2008; Arraut and Satyamurty, 2009; Dirmeyer et
19 al., 2009; Van der Ent et al., 2010; Keys et al., 2012; Spracklen et al. 2012; Bagley et
20 al., 2014), the contribution from the basin predominantly extends towards southeastern
21 South America (including the La Plata Basin, hereafter LP). Moisture is also transported
22 towards southeastern Brazil during the austral Spring and the summer months, a period
23 characterised by the active phase of the SAMS(Vera et al., 2006). The Orinoco Basin,
24 the Atlantic ITCZ, and part of the Caribbean Sea also receive some moisture from the
25 Amazon region, except during the austral summer. This can probably be explained in

terms of the positioning of the VIMF convergence associated with the ITCZ in the northern latitudes for most of the year, enhancing the moisture transport from Amazon towards these sinks (Figure 1, right-hand column). Using a different data set and analysing a 5-year period, Nieto et al. (2008) verified some contribution of moisture from the Amazon into the Orinoco during the months of JJAS, a period characterised by drought conditions in the southern Amazon. Moisture from the Amazon is also transported towards parts of the Pacific ITCZ and the Western Hemisphere Warm pool (Drumond et al., 2011, and references quoted therein) regions. Figure 3 also suggests some recycling throughout the year, with local moisture sink areas expanding over the central and southern basin from September to April, while reducing in extent towards the northern and southern basin from May to August.

In order to investigate the annual cycle of the contribution from the Amazon towards the LP region, a similar analysis to that applied to the backward case was performed for the forward case. As previously explained, the boundaries of the LP box (67–50°W; 20–34°S) were defined according to the contour line of -0.4 mm day^{-1} in the 33-year annual average of the 10-day integrated ($E - P$) values of the forward trajectories from the Amazon Basin (Fig. 4a). Here, -0.4 mm.day^{-1} corresponds to the 95% percentile of all the negative values obtained. We integrated the monthly averages of the 10-day ($E - P$) forward trajectories shown in Fig. 3 over the LP area, and in order to present the results as clearly as possible Fig. 4b shows the absolute values of ($E - P$), because all values obtained over the area are negative ($(E - P) < 0$, meaning that LP acts as a sink of moisture from the Amazon throughout the year). Figure 4b suggests a higher-frequency variability of the moisture contribution (presenting something like a seasonal cycle) superimposed on an annual cycle with maximum values during the austral

1 spring/summer and minima during autumn/winter. It shows maximum contributions
2 during June (a secondary maximum), October and January, and minima in August,
3 December (a secondary minimum) and March. The migration of the ITCZ associated
4 with the development of the SAMS may explain the annual cycle of the moisture
5 contribution from the Amazon for LP. According to previous studies (e.g., Moura and
6 Shukla, 1981; Folland et al., 1986), the Atlantic ITCZ presents a seasonal latitudinal
7 migration coupled with the annual cycle of the spatial distribution of the maximum SST
8 observed over the TA, and it reaches its maximum northward (southward) displacement
9 during austral spring (autumn). However, the causes of this near-seasonal variability
10 remain unclear for us and merit further attention. The VIMF analysis shown in Figure 1
11 suggests some monthly variability in the moisture flux from the Amazon towards LP,
12 which then leads to the configuration of different patterns of convergence or divergence
13 of VIMF over the target region throughout the year.

15 *3.2 Role of ENSO on the moisture transport over the Amazon basin*

17 Figure 5 shows the differences in the composites of moisture sources of the Amazon
18 Basin for El Niño and La Niña events. Both composite fields were obtained considering
19 only positive ($E-P$) values (source regions) obtained in the backward analysis. Now,
20 pink (green) colours indicate regions where their contribution as a source intensified
21 during El Niño (La Niña) events. From the results it is clear that the moisture
22 contribution from the equatorial Atlantic was enhanced during all months of an El Niño
23 cycle. In comparison to La Niña episodes, it seems that the contribution from the
24 Tropical and Subtropical Atlantic was weakened during an El Niño cycle. The
25 differences in the VIMF from both composites (Figure 5, right-hand column) show

enhanced VIMF divergent conditions over the equatorial Atlantic during the El Niño episodes selected, accompanied by an intensified moisture transport from there towards the basin. However, the enhanced VIMF divergence expanding towards tropical South America probably inhibited the precipitation of the moisture carried from the ocean to the Amazon. We believe that the configuration of these patterns may be understood through the displacement of the Walker cell eastwards as observed during an El Niño cycle, favouring subsidence over tropical South America. As a probable consequence of the presence of this intensified subsidence over the continent, the VIMF differences suggest the displacement of the moisture flux convergence associated with the Atlantic ITCZ northwards during April and May (year 1), probably associated with the inhibition of the latitudinal ITCZ migration southwards. The known importance of the ENSO in modulating South American precipitation through its associated changes in atmospheric circulation (e.g. Kousky et al, 1984; Ropelewski and Halpert, 1987) was also reported in a correlation analysis by Van der Ent and Savenije (2013).

Looking at La Niña cycle (Figure 5, green colours), from June to October (year 0) there was an enhancement of the Southern Atlantic source associated with a higher contribution from the southern Amazon. These anomalous patterns weakened during November and December (year 0), being replaced by increased sources over the La Plata basin, over the western continent, and over the northern Atlantic. During January and February (year 1) the anomalous sources weakened over the western continent, while they were enhanced over the tropical northern and southern Atlantic domains. The anomalous North Atlantic source persisted until May (year 1), while the anomalous South Atlantic reduced in size during February - April (year 1). The anomalous contribution from the La Plata basin disappeared from February (year 1) onwards.

1

2 If we analyse the variability of ($E-P$) integrated over the NA and TA boxes during the
3 ENSO cycle using a composite analysis (Fig. 2b, green and pink lines indicate the
4 contribution during La Niña and El Niño years, respectively), the contribution from the
5 NA presents a slight increase (decrease) from June (year 0) to January (year 1) for El
6 Niño (La Niña) years with respect to the climatology. Then, there is a reverse in the
7 signal of the NA anomalies, and the contribution from this box region towards the
8 Amazon basin decreases (increases) during FMAM (year 1) of an El Niño (La Niña)
9 event. The VIMF differences (Figure 5, right-hand column) may illustrate some aspects
10 of the variability of the NA contribution. The positioning of the NA box coincides with
11 the region of increased VIMF divergence observed over the Equatorial Atlantic during
12 the first months of an El Niño cycle. It may explain the higher moisture contributions
13 from this box to the Amazon. However, it seems that the location of NA coincides with
14 the anomalous Atlantic ITCZ displaced northwards during the austral autumn. A
15 reduction in the moisture contribution from this box is then a plausible consequence. In
16 comparison to the NA, the anomalies of the SA contribution present higher variability in
17 their signal during an ENSO cycle. Some increase in the SA contribution prevails from
18 September (year 0) to February (year 1) during La Niña events. Figure 2b also indicates
19 the change in the signal of the anomalies over the SA boxes at the end of the ENSO
20 cycle. This means that during an El Niño (a La Niña) event, the contribution from the
21 SA is enhanced (decreased) from February (year 1) onwards. Doubtless as a result of
22 the inhibition of the Atlantic ITCZ southwards during the austral autumn of an El Niño
23 cycle, an intensified VIMF divergence (Figure 7, right-hand column) was configured in
24 the SA region, from where the moisture transport was intensified towards the Amazon.

25

1 If we consider the six flood years in the Amazon (1988/89, 1993/94, 1998/99, 2008/09,
2 2010/11, 2011/2012) and five drought years (1979/80, 1982/83, 1997/98, 2004/05,
3 2009/10) identified from the previous studies of Marengo et al. (2013a; 2013b), the
4 anomalous contributions from the SA and the NA boxes verified in the ENSO events
5 are quite similar to the anomalous transports during these drought and flood episodes
6 (figure not shown). This may be explained due to the strong similarity of the elements
7 selected for both composites. Only one (1993/94) of the six flood years identified was
8 associated with neutral ENSO conditions, while the other events took place during La
9 Niña episodes. The same occurred for drought years: only one (1979/80) of the five
10 episodes did not take place during El Niño conditions.

11 In the search for some interannual joint variability between ENSO and the contribution
12 from the two sources, a correlation analysis was undertaken between the monthly time
13 series of ONI and of $(E-P)$ integrated over each box. The correlations are indicated in
14 Table 1, and only those coefficients significant at the 90% level according to the T-
15 Student test are discussed. In view of the linear relationship between the ENSO and the
16 NA time series, the negative correlation for MAM implies that during La Niña (El
17 Niño) events the contribution from NA to the Amazon basin increases (decreases), in
18 accordance with Figure 2b. The positive correlation obtained during the period from
19 June to October might have some influence on the establishment of the transition phase
20 of the role of the NA as a moisture source (climatologically it occurs during
21 September). When we consider the contribution of SA, the positive ONI/SA correlation
22 coefficients observed during MAM imply that the contribution from the SA towards the
23 Amazon increases (decreases) during El Niño (La Niña) events, in accordance with the
24 results shown in Figure 2b. The negative ONI/SA correlations observed in September
25 and January mean that the contribution from the SA increases (decreases) during La

Niña (El Niño) events. A comparison of the results obtained for the two boxes reveals that the NA and the SA present opposite behaviour in terms of their joint linear variability with the ENSO, except during June and July when both indexes show positive correlation coefficients. During Spring, the contribution from NA increases during El Niño events, while that from SA reduces during September. We do not intend to address it here, but a theme worthy of investigation in more detail in future work is the possible role of the interaction between the ENSO and the NA and SA contributions on the onset of the active phase of SAMS during austral spring (Vera et al., 2006). Furthermore, autumn is the season with the most contrasting coefficients, and this coincides with the peak of the rainy season in the Amazon Basin. While the contribution from SA increases in MAM during El Niño events, the contribution from NA reduces.

In order to investigate the impact of the ENSO on moisture transport from the Amazon, Figure 6 shows the differences in the composites of the moisture sinks for El Niño and La Niña events. In the composite figures we considered only negative ($E-P$) values (sink regions) obtained in the forward analysis from the basin. The pink (green) colours indicate regions where the moisture sinks intensified during El Niño (La Niña) events. It seems that the transport from the Amazon was enhanced towards southeastern South America (particularly the La Plata Basin) during the beginning of the El Niño phase, and this anomalous sink is displaced northwards during the cycle. The VIMF differences (Figure 5, right-hand column) reveal the predominance of intensified moisture transport towards the subtropics and enhanced moisture flux convergence over southeastern South America during an El Niño cycle. During the onset of El Niño events (from June to August in year 0), the moisture contribution increased towards the northwestern Amazon and the Pacific ITCZ (pink colour), and this last region acted

again as an anomalous sink from February to April (year 1). Again, the VIMF differences suggest some moisture transport towards the Pacific ITCZ, particularly from November (year 0) onwards. This might be understood via the eastward displacement of the Walker cell, increasing precipitation over the eastern equatorial Pacific. Instead, moisture transport is enhanced towards northwestern South America and the Atlantic ITCZ during the onset of La Niña events (from June to September in year 0, green colour). From the austral spring onwards for La Niña events, the moisture transport was enhanced towards the tropical latitudes. The anomalous patterns of moisture transport from the Amazon indicated in this figure are in accordance with the precipitation anomalies observed during El Niño: precipitation displaced from the tropical region towards the La Plata Basin and drought conditions over the Northern continent (Vera et al., 2006).

The variability of the contribution from the Amazon basin towards LP during an ENSO cycle as obtained using our composite analysis is quantified in Figure 4b, in which the green and pink lines indicate the contribution during La Niña and El Niño years, respectively. This figure confirms the changes in the transport towards the tropics or subtropics according to the ENSO phase, as discussed in the previous paragraph. In general, the contribution towards LP increases during El Niño episodes, particularly during July (year 0), October (year 0) - January (year 1), and March-May (year 1). The increased contribution towards LP between October (year 0) and January (year 1) for El Niño events coincides with the slight greater supply of moisture from NA towards the Amazon (Fig. 2b) observed during these years. However, the increased contribution from the Amazon towards LP during March-May (year 1) coincides with a higher supply from the SA (Fig 2b). The results for the La Niña composite indicate a reduction

1 in the contribution from the Amazon towards LP, particularly during October-December
2 (year 0) and March-May (year 1). The linear correlation analysis applied between the
3 time series of ONI and of absolute values of ($E-P$) from the forward experiment
4 integrated over LP (table 1) shows the predominance of positive correlation coefficients,
5 presenting higher values in October-December (year 0) and April-May (year 1). This
6 indicates that during El Niño (La Niña) events the supply of moisture from the Amazon
7 basin towards LP is enhanced (reduced), in agreement with the results obtained from the
8 composite analysis (Fig 4b).

9
10 In a tentative summary of the main results obtained from the composites and linear
11 correlation analyses, it seems that the moisture contribution from NA was enhanced
12 towards the Amazon basin during June-October (year 0) for El Niño episodes, as well as
13 some increase in the transport from SA during June-July (year 0). This suggests that
14 moisture transport towards the basin was more associated with the ENSO during the
15 pre-monsoon period. Nevertheless, the ENSO episodes are associated more with the
16 transport from the Amazon towards LP during the monsoon active phase (from October
17 year 0 onwards).

18 19 *3.3 Role of the AMM in the moisture transport over the Amazon basin*

20

21 Although almost all the drought and flood years identified by Marengo et al. (2013a;
22 2013b) were associated with ENSO extreme episodes, it is interesting to note that two
23 of them occurred during neutral ENSO conditions. This suggests an effect of other
24 climatic modes on the variability of precipitation in the basin. When we considered the
25 tropical Atlantic, we found that these two episodes were related to extreme AMM

conditions. Moreover, three of the six flood years selected by Marengo et al. occurred during AMM episodes (1988/89, 1993/94 and 2008/09), while three of the five drought years were associated with AMM+ events (1979/80, 1982/83, 2009/2010). We must stress that not all the extreme AMM episodes selected were related to the drought and flood years investigated: only three of the seven AMM+(-) episodes were drought-(flood)-years. Previous studies reported some related variability of the SST anomalies over the equatorial Pacific and tropical Atlantic oceans characterised by El Niño and AMM+ conditions (and vice-versa) (e.g., Chang et al., 2001; Czaja et al., 2002; Melice and Servain, 2003), in partial agreement with our results: three (two) drought (flood) years were observed during El Niño/AMM+ (La Niña/AMM-) conditions. In particular, in agreement with the present results, Souza et al (2005) also analyzed the two extreme and contrasting climatic scenarios, defined as UNFAV (UNFAVorable - simultaneous manifestations of the El Niño and AMM+) and FAV (FAVorable - concomitant occurrence of the La Niña and AMM-). UNFAV (FAV) composites for unfiltered austral autumn data showed outstanding changes in both the Walker and Hadley cells in association with anomalous weakening (enhanced) in the Atlantic ITCZ that, in consequence, yields deficient (abundant) rainfall in most of the East Amazon and Northeast Brazil. However, it seems that anomalous Atlantic conditions accompanied by a neutral ENSO phase can also be associated with extreme precipitation years in the Amazon.

Figure 7 shows the temporal evolution of the differences in AMM+ and AMM- composites of moisture sources of the Amazon Basin over the year (left-hand columns). Again, both composite fields were established considering only positive ($E-P$) values (source regions) obtained in the backward analysis. Pink (green) colours reveal regions where the contribution of a source intensified during AMM+ (AMM-) years. When we compare the two cases, it seems that an anomalous see-saw structure of the moisture

1 sources prevailed during FMAM (year 1), with the South (North) Atlantic region
2 increasing its contribution towards the Amazon during AMM+(-) episodes. Considering
3 the VIMF differences for the two composites (Figure 7, right-hand column), a cyclonic
4 structure configured over the northern hemisphere suggests the weakening of the Azores
5 High from December (year 0) onwards for AMM+ episodes. VIMF convergence was
6 then favoured over an area covering the eastern and tropical North Atlantic, and from
7 January (year 1) onwards a dipolar structure was configured over the tropical Atlantic,
8 increasing convergent conditions over NA and divergence over SA. This pattern agrees
9 with the source analysis discussed above, and suggests the displacement of the Atlantic
10 ITCZ northwards during the AMM+ events studied. From the same figure it is possible
11 to identify the intensification of the moisture transport from SA towards the Amazon,
12 probably due to enhanced VIMF convergent conditions configured over the Eastern
13 Equatorial Pacific and the north of the continent during the AMM+ phase. In April
14 (year 1) of the same episodes, an anticyclonic structure was favoured over central South
15 America, and this probably reinforced the moisture transport from SA towards the
16 Amazon, as well as the transport from the basin towards the subtropics. Considering
17 only the AMM- years, the results suggest changes in the structure of the anomalous
18 moisture sources over the months of interest. While the moisture contribution prevailed
19 from the equatorial and southern tropical Atlantic regions from June to November (year
20 0; green colours), anomalous transport was displaced towards the North Atlantic region
21 from December (year 0) onwards. During AMM+ years, it seems that some moisture
22 was contributed by the basin itself from June to October (year 0). Afterwards, the
23 anomalous source extended its domain towards northern South America, as well as to
24 the equatorial and the southern tropical Atlantic regions. A similar evolution in the
25 enhanced VIMF divergence extending from eastern Amazon basin towards the tropical

Atlantic during the AMM+ phase agrees with the enhanced importance of these areas as moisture sources for our target area.

If we consider the variability of ($E-P$) integrated over the NA and the SA regions during the years of extreme of AMM (Fig. 2c, green and pink lines indicate the contribution during AMM- and AMM+ events, respectively), it seems that the major changes in the contribution from the two sources compared with the climatology occur from December (year 0) onwards. Confirming the see-saw structure identified in Figure 7, it seems that the contribution from NA increased (decreased) and that from SA decreased (increased) during AMM- (+) episodes. Such a relationship tallies with the linear correlation analysis between the AMM and the NA and the SA time series shown in the Table 1.

In order to investigate possible changes in the moisture transport from the basin associated with extreme AMM years, Figure 8 shows the differences in the positive and negative AMM phase composites of the moisture sinks in the Amazon. Here, the pink (green) colours indicate regions where moisture sinks intensify during AMM+ (-) years. These results suggest some monthly variability in the preferred sinks. Nevertheless, it seems that moisture transport intensified towards the subtropical South America (the Amazon and northeastern Brazil) during the AMM+ (-) phase, particularly from October (year 0) onwards. From June to September (year 0) the anomalous patterns were mixed, but they suggest some presence of anomalous sinks over the western (eastern) Amazon and subtropical (extratropical) South America during AMM+(-) events. Transport was also favoured towards northwestern South America and the Pacific ITCZ during the austral spring of each AMM+ episode. All these patterns may also be identified via VIMF analysis (Figure 7, right-hand column): during the AMM+

1 phase, VIMF convergent conditions predominated over the subtropical South America
2 (with some temporal variation in the spatial domain), and over the eastern equatorial
3 Pacific and northwestern continental areas.

4
5 The variability in the anomalous contribution from the Amazon basin towards LP
6 during extreme AMM years is quantified in Figure 4c, where the green and pink lines
7 indicate the contribution during AMM- and AMM+ years, respectively. It is interesting
8 to note that the anomalous contribution towards LP presents variability over the year:
9 this increased (reduced) during the periods October (year 0)-January (year 1) and April-
10 May (year 1) in AMM+ (-) years. This is probably associated with the temporal
11 variations in the location of the intensified VIMF convergent subtropical nuclei as
12 verified in Figure 7. The correlation analysis presented in Table 1 confirms that there is
13 a significant linear relationship between the AMM and the contribution towards LP only
14 during April-May (year 1).

16 **4. Conclusions**

17
18 An analysis of the moisture sources for the Amazon basin, as well as its role as a source
19 of humidity, was performed using a Lagrangian method of diagnosis through numerical
20 experiments with the FLEXPART model and the ERA-Interim data set. The
21 climatological annual cycle of the main moisture sources and sinks of the Amazon was
22 characterised for the period June 1979 to May 2012. The large temporal domain (33-
23 year) allowed the investigation of some aspects of the interannual variability of the
24 moisture transport over the basin, such as the role of the anomalous SST conditions in
25 the Pacific and the Atlantic on the Amazonian hydrological budget.

1

2 The results obtained show the role of the Tropical Atlantic as a remote source of

3 moisture for the Amazon Basin. The northern tropical Atlantic (the NA) contributes

4 mainly during the extended austral summer, and this region does not act as a moisture

5 source for the Amazon basin between June and September, and the transition

6 sink/source of the role of the NA occurs in September. On the other hand, the

7 contribution of the southern tropical Atlantic (the SA) occurs all year round and

8 predominates from April to November, reaching its maximum during the austral winter.

9 Considering the Amazon basin as a source of moisture, the main contribution from the

10 Amazon occurs for southeastern South America throughout the year and also for

11 southeast Brazil during the austral spring and summer months. The Orinoco basin and

12 the Pacific ITCZ also receive some moisture from the Amazon region, except during the

13 austral summer.

14

15 A classification of the severe years according to the ENSO and AMM conditions

16 suggests that the drought years identified by Marengo et al. (2013a; 2013b) coincided

17 with El Niño and/or AMM+ phases, and vice-versa. Concerning the role of the ENSO

18 and AMM climatic modes on the interannual variability of the moisture transport over

19 the Amazon, it seems that the ENSO is more associated with the interannual variability

20 of the NA contribution during the months before the peak of the rainy season in the

21 basin (FMAM), and El Niño events enhance the transport from this source towards the

22 basin. During FMAM, both ENSO and AMM modes are associated with the interannual

23 variability of the contribution from the sources, although correlation analysis suggests

24 that the linear relationship with AMM is higher. La Niña episodes accompanied with

25 negative AMM conditions were associated with a higher contribution from NA in these

1 months. For the variability of the SA source, the results suggest some linear association
2 with ENSO and particularly with AMM during FMAM, and El Niño (La Niña) episodes
3 with AMM + (AMM -) events were associated with enhanced transport from SA. If we
4 consider the transport from the basin towards LP, it seems that the ENSO has a stronger
5 linear association, and El Niño (La Niña) episodes were associated with higher
6 (reduced) contributions.

7
8 In summary, the results from the composites and the linear correlation analyses suggest
9 that during the peak of the rainy season (FMAM) the AMM is associated more with the
10 interannual variations in the contribution from both the tropical Atlantic sources, while
11 the transport from the basin towards the LP responds more to the ENSO variability. It
12 seems that in the absence of an anomalous mechanism of moisture transport from the
13 Amazon towards the subtropics during neutral ENSO years, the anomalies of moisture
14 in the basin are associated with the role of the AMM in the contribution from the
15 oceanic climatological sources. Unfortunately, the extreme drought/flood year sample is
16 small and only two episodes were configured during neutral ENSO years, which renders
17 our statements inconclusive. The use of dynamical climatic models to investigate the
18 joint role of the ENSO and the AMM on the hydrological budget of the basin during
19 these Amazon drought/flood years may address this lack of data and help us to
20 understand the mechanisms involved in the variations in moisture transport.

21 22 **Acknowledgements**

23
24 Anita Drumond, Raquel Nieto and Luis Gimeno acknowledge the support from the
25 Spanish Government and FEDER through the project TRAMO. Tercio Ambrizzi and

Jose Marengo would like to acknowledge the contribution of the Rede Clima, Brazilian National Institute of Science and Technology (INCT) for Climate Change, funded by CNPq Grant Number 573797/2008-0 and FAPESP Grant Numbers 2008/57719-9, 2008/58101-9, 2008/58161-1 and Go Amazon 2013/50538-7. We acknowledge the suggestions of the Editor and of the Anonymous Reviewers.

References

Angelini, I. M., and Coauthors, 2011: On the coupling between vegetation and the atmosphere. *Theor. Appl. Climatol.*, 105, 243–261, doi:10.1007/s00704-010-0377-5.

Arraut, J.M., Nobre, C., Barbosa, H. M. J., Obregon, G., Marengo, J.: Aerial Rivers and Lakes: Looking at Large-Scale Moisture Transport and Its Relation to Amazonia and to Subtropical Rainfall in South America, *J. Climate*, 25, 543–556, doi: <http://dx.doi.org/10.1175/2011JCLI4189.1>, 2012.

Arraut, J.M., Satyamurty, P.: Precipitation and Water Vapor Transport in the Southern Hemisphere with Emphasis on the South American Region, *J. App.Meteor. Cli.*, 48, 1902-1912, doi: 10.1175/2009JAMC2030.1, 2009.

Bagley, J.E., Desai, A.R., Harding, K.J., Snyder, P.K., Foley, J.A.: Drought and deforestation: Has land cover change influenced recent precipitation extremes in the Amazon?, *J. Climate*, 27, 345-361, DOI: 10.1175/JCLI-D-12-00369.1, 2014.

1 Bengtsson, L., Hagemann, S., and Hodges, K. I.: Can climate trends be calculated from
2 reanalysis data?, J. Geophys. Res., 109, doi:10.1029/2004JD004536, 2004.

3

4 Bosilovich, M.G., Chern, J.-D.: Simulation of water sources and precipitation recycling
5 for the MacKenzie, Mississippi, and Amazon river basins, J. Hydrometeor., 7, 312-329,
6 2006

7

8 BRUBAKER, K.L.; ENTEKHABI, D.; EAGLESON, P.S.: Estimation of continental
9 precipitation recycling, J. Climate, v.6, p. 1077-1089, 1993.

10

11 Carvalho, L.M.V., Silva, A.E., Jones, C., Liebmann, B., Silva Dias, P.L., Rocha, H.R.:
12 Moisture transport and intraseasonal variability in the South America monsoon system,
13 Climate Dynamics, 36, 1865-1880, 2011.

14

15 Chang, P, L Ji, R Saravanan: A hybrid coupled model study of tropical Atlantic
16 variability. J Clim, 14, 361-390, 2001.

17

18 Coe, M., Costa, M.H., Botta, A., Birkett, C.: Long term simulations of discharge and
19 floods in the Amazon river, J. Geophys. Res., 107, 11-1,11-17, 2002.

20

21 Costa, M.H., Foley, J.A.: Trends in the hydrologic cycle of the Amazon basin, J.
22 Geophys. Res., 104, 14189-14198, 1999.

23

24 Czaja, A, P van der Vaart, J Marshall: A diagnostic study of the role of remote forcing
25 in tropical Atlantic variability. J Clim, 15, 3280-3290, 2002.

Dee, D., et al.: The ERA Interim reanalysis: Configuration and performance of the data assimilation system, *Quart. J. Roy. Meteor. Soc.*, 137, 553–597, doi:10.1002/qj.828, 2011.

Dirmeyer, P. A, Schlosser, C. A., Brubaker, K. L.: Precipitation, Recycling, and Land Memory: An Integrated Analysis, *J. Hydrometeor.*, 10, 278-288, DOI:10.1175/2008JHM1016.1, 2009.

Dirmeyer, P. A., and Brubaker, K. L.: Characterization of the global hydrologic cycle from a back-trajectory analysis of atmospheric water vapor, *J. Hydrometeorol.*, 8(1), 20–37, 2007.

Drumond, A., Nieto, R., Gimeno, L.: On the contribution of the Tropical Western Hemisphere Warm Pool source of moisture to the Northern Hemisphere precipitation through a Lagrangian approach, *J. Geophys. Res.*, 116, D00Q04, doi: 10.1029/2010JD015397, 2011.

Drumond, A., Nieto, R., Gimeno, L., Ambrizzi, T.: A lagrangian identification of major sources of moisture over Central Brazil and La Plata Basin, *J. Geophys. Res.*, 113, D14128, doi: 10.1029/2007J009547, 2008.

ELTAHIR, E. A. B.; BRAS, R. L.: Precipitation recycling in the Amazon Basin. *Quart. J. Roy. Met. Soc.* v. 120, p. 861-880, 1994.

1 Folland, C, Parker, P.D.: Sahel rainfall and worldwide surface temperatures: 1901-
2 1985. *Nature*, 320, 602-606, 1986.

3
4 Foley, J.A., Botta, A., Coe, M.T., Costa, M.H.: El Niño-Southern Oscillation and the
5 climate, ecosystems and rivers of Amazonia, *Global Biogeochem. Cycles*, 16(4), 1132-
6 1144, 2002.

7
8 Gat, J. R., Matsui, E.: Atmospheric water balance in the Amazon basin: An isotopic
9 evapotranspiration model, *J. Geophys. Res.*, 96(D7), 13179–13188,
10 doi:10.1029/91JD00054, 1991.

11
12 Gimeno, L., Nieto, R., Drumond, A., Castillo, R., Trigo, R.: Influence of the
13 intensification of the major oceanic moisture sources on continental precipitation, *Geo.*
14 *Res. Lett.*, 40, 1-8, doi: 10.1002/grl.50338, 2013.

15
16 Gimeno, L. et al.: Oceanic and Terrestrial Sources of Continental Precipitation, *Rev.*
17 *Geophys.* doi:10.1029/2012RG000389, 2012.

18
19 Grimm, A.M.; Ambrizzi, T.. Teleconnections into South America from the Tropics and
20 Extratropics on Interannual and Intraseasonal Timescales. In: Françoise Vimeux;
21 Florence Sylvestre; Myriam Khodri. (Org.). *Past Climate Variability in South America*
22 *and Surrounding Regions*. Netherlands: Springer Netherlands, v. 14, p. 159-191, 2009.

23
24 Keys, P.W., van der Ent, R.J., Gordon, L.J., Hoff, H., Nikoli, R., Savenije, H.H.G.:
25 Analyzing precipitation sheds to understand the vulnerability of rainfall dependent
26 regions, *Biogeosciences*, 9, 733-746, DOI: 10.5194/bg-9-733-2012, 2012.

Knippertz, P., Wernli, H., Glaser, G.: A global climatology of tropical moisture, *J. Clim.*, 26, 3031–3045, doi:10.1175/JCLI-D-12–00401.1, 2013.

Kousky V. et al: A review of the Southern Oscillation: oceanic-atmospheric circulation changes and related rainfall anomalies, *Tellus*, 36A, 490-504, 1984.

Lewis, S.L., Brando, P.M., Phillips, O.L., van der Heijden, G. M. F., Nepstad, D.: The 2010 Amazon Drought, *Science*, 331, doi: 10.1126/science.1200807, 2011.

Liebmann, B., Marengo, J.A.: Interannual Variability of the Rainy Season and Rainfall in the Brazilian Amazon Basin. *J. Climate*, 14, 4308–4318. doi: [http://dx.doi.org/10.1175/1520-0442\(2001\)014<4308:IVOTRS>2.0.CO;2](http://dx.doi.org/10.1175/1520-0442(2001)014<4308:IVOTRS>2.0.CO;2), 2001.

Makarieva, A. M., V. G. Gorshkov, D. Sheil, A. D. Nobre, and B. L. Li, 2013: Where do winds come from? A new theory on how water vapor condensation influences atmospheric pressure and dynamics. *Atmos. Chem. Phys.*, 13, 1039–1056, doi:10.5194/acp-13-1039-2013.

Marengo, J.A.: The characteristics and variability of the atmospheric water balance in the Amazon basin: Spatial and temporal variability, *Climate Dynamics*, 24, 11-22, 2005.

Marengo, J.A.: ON THE HYDROLOGICAL CYCLE OF THE AMAZON BASIN: A HISTORICAL REVIEW AND CURRENT STATE-OF-THE-ART, *Revista Brasileira de Meteorologia*, v.21, n.3, 1-19, 2006

1

2 Marengo, J. A., Borma, L.S., Rodriguez, D. A., Pinho, P., Soares, W. R., , Alves, L.M.:

3 Recent Extremes of Drought and Flooding in Amazonia: vulnerabilities and human

4 adaptation, AJCC, 2, 87-96. doi: <http://dx.doi.org/10.4236/ajcc.2013.22009>, 2013a.

5

6 Marengo, J. A., Alves, L. M., Soares, W. R., Rodriguez, D. A., Camargo, H., Riveros,

7 M. P., Pabló, A. D.: Two Contrasting Severe Seasonal Extremes in Tropical South

8 America in 2012: Flood in Amazonia and Drought in Northeast Brazil, J. Climate, 26,

9 9137–9154. doi: <http://dx.doi.org/10.1175/JCLI-D-12-00642.1>, 2013b.

10

11 Marengo, J., Nobre, C.: Clima da regio Amazonica, In: Tempo e clima no Brasil,

12 Cavalcanti, I.F.A et al. eds., Oficina de Textos, Sao Paulo, Brazil, 197-212. In

13 Portuguese, 2009.

14

15 Marengo, J.A, Nobre, C.A., Tomasella, J., Oyama, M.D., Oliveira, G.S., Oliveira, R., et

16 al.: The drought of Amazonia in 2005, Journal of Climate, 21(3), 495-516, 2008.

17

18 Marengo, J.A, Liebmann, B., Kousky, V., Filizola, N., Wainer, I.: Onset and end of the

19 rainy season in the Brazilian Amazon basin, Journal of Climate, 14, 833-852, 2001.

20

21 Melice, J.L., Servain, J, 2003: The tropical Atlantic meridional SST gradient index and

22 its relationships with SOI, NAO and the Southern Ocean. Clim Dyn, 20, 447-464.

23

24 MOLION, L. C. B.: A climatonic study of the energy and moisture fluxes of the

25 Amazon basin with considerations of deforestation effects. Ph. D. thesis. University of

26 Wisconsin, Madison, 1975.

1
2 Moura, AD, Shukla, J,: On the dynamics of droughts in northeast Brazil: observations,
3 theory and numerical experiments with a general circulation model. JAS, 38, 2653-
4 2675, 1981

5
6 Nieto, R., Gallego, D., Trigo, R. M., Ribera, P., Gimeno, L.: Dynamic identification of
7 moisture sources in the Orinoco basin in equatorial South America, Hydrological
8 Sciences-Journal des Sciences Hydrologiques, 53, (3), 602-617, 2008.

9
10 NÓBREGA, R.S.; CAVALCANTI, E.P.; SOUZA, E.P. Reciclagem de vapor d'água
11 sobre a América do Sul utilizando reanálises do NCEP-NCAR. Revista Brasileira de
12 Meteorologia, v.20, n.2, p.253- 262, 2005.

13
14 Numaguti, A.: Origin and recycling processes of precipitating water over the Eurasian
15 continent: Experiments using an atmospheric general circulation model, J. Geophys.
16 Res. 104, 1957–1972, 1999.

17
18 Rayner, N. A., Parker, D. E., Horton, E. B., Folland, C. K., Alexander, L. V., Rowell,
19 D. P., Kent, E. C., Kaplan, A.: Global analyses of sea surface temperature, sea ice, and
20 night marine air temperature since the late nineteenth century, J. Geophys. Res., 108,
21 D14, 4407 10.1029/2002JD002670 , 2003

22
23 Richey, J., Nobre, C.A., Deser, C.: Amazon river discharge and climate variability:
24 1903 to 1985, Science, 246, 101-103, 1989.

Roads, J., Kanamitsu, M., Stewart, R.: Water and energy budgets in the NCEP-DOE reanalyses, *J. Hydrometeor.*, 3(3), 227-248, 2002.

Ropelewski and Halpert: Global and Regional Scale Precipitation Patterns Associated with the El Niño/Southern Oscillation. *Monthly Weather Review*, 115, 1606- 1626, 1987.

Ruiz-Barradas, A, JA Carton, S Nigam: Structure of interannual-to-decadal climate variability in the Tropical Atlantic sector. *J Clim*, 13, 3285-3297, 2000.

SALATI, E.: The Forest and the Hydrological Cycle, J. H. Gash, C. A. Nobre, J. M. Roberts, and R. L. Victoria, editors. *Amazonian deforestation and climate*. John Wiley and Sons, Chichester, UK, p. 273-296, 1987.

Satyamurty, P., da Costa, C.P.W., Manzi, A.O., Candido, L.A.: A quick look at the 2012 record flood in the Amazon Basin, *Geo. Res. Lett.*, 40, 1396-1401, doi: 10.1002/grl.50245, 2013.

Satyamurty, P., da Costa, C.P.W., Manzi, A.O.: Moisture source for the amazon Basin: a study of contrasting years, *Theor. Appl. Climatol*, 111, 195-209, doi: 10.1007/s00704-012-0637-7, 2013

Servain J.: Simple climatic indices for the tropical Atlantic Ocean and some applications. *Journal of Geophysical Research*, 96, 15 137–15 146, 1991.

SILVA, A.E. Variabilidade da Circulação e Transporte de Umidade no Regime de Monção da América do Sul. 2009. 137f. Tese (Doutorado) – Instituto de Astronomia, Geofísica e Ciências Atmosféricas, Universidade de São Paulo, São Paulo, 2009.

Smith, T.M., Reynolds, R.W., Peterson, T.C., Lawrimore, J.: Improvements to NOAA's Historical Merged Land-Ocean Surface Temperature Analysis (1880-2006), Journal of Climate, 21, 2283-2296, 2008.

Souza, E. B. ; Kayano, M. T.; and Ambrizzi, T.: Intraseasonal and submonthly variability within autumn rainy regime over the Eastern Amazon/Northeast Brazil and associated atmospheric mechanisms.. Theoretical And Applied Climatology, Austria, v. 81, n.3-4, p. 177-192, 2005.

Spracklen, D.V., Arnold, S.R., Taylor, C.M.: Observations of increased tropical rainfall preceded by air passage over forests, Nature, doi: 10.1038/nature11390, 2012.

Sternberg, H.R.: Aggravation of floods in the Amazon River as a consequence of deforestation? Geografiska Annaler, 69A, 201-219, 1987.

Stohl, A., James, P.: A Lagrangian analysis of the atmospheric branch of the global water cycle. Part 1: Method description, validation, and demonstration for the August 2002 flooding in central Europe, J. Hydrometeor., 5, 656– 678, 2004.

1 Stohl, A., James, P.: A Lagrangian analysis of the atmospheric branch of the global
2 water cycle: 2. Earth's river catchments, ocean basins, and moisture transports between
3 them, *J. Hydrometeor.*, 6, 961–984, 2005.

4
5 Trenberth, K. E.: The Definition of El Niño, *Bulletin of the American Meteorological*
6 *Society*, 78(12), 2771-2777, 1997.

7
8 TRENBERTH, K.E. Atmospheric Moisture Recycling: Role of Advection and Local
9 Evaporation. *J Climate*, v.12, n.5, p.1368-1381, 1999.

10
11 Uvo, C.R.B., Repelli, C.A., Zebiak, S., Kushnir, Y.: The relationship between tropical
12 Pacific and Atlantic SST and Northeast Brazil monthly precipitation, *Journal of*
13 *Climate*, 11, 551-562, 1998.

14
15 van der Ent, R. J., Savenije, H. H. G.: Oceanic sources of continental precipitation and
16 the correlation with sea surface temperature, *Water Resour. Res.*, 49 (7), 3993-4004,
17 doi:10.1002/wrcr.20296, 2013.

18
19 van der Ent, R. J., Savenije, H. H. G., Schaeffli, B., and Steele-Dunne, S. C.: Origin and
20 fate of atmospheric moisture over continents, *Water Resour. Res.*, 46, W09525,
21 doi:10.1029/2010WR009127, 2010.

22
23 Vera, C., et al.: A unified view of the American monsoon systems, *J. Clim.*, 19, 4977–
24 5000, 2006.

1 Wei, J., Dirmeyer, P. A., Bosilovich, M. G., and Wu, R.: Water vapor sources for
2 Yangtze River Valley rainfall: Climatology, variability, and implications for rainfall
3 forecasting, *J. Geophys. Res.*, 117, D05126, doi:10.1029/2011JD016902, 2012.

4
5 Williams, E., Dall'antonia, A., Dall'antonia, V., de Almeida, J.M., Suarez, F.,
6 Liebmann, B., Malhado, A.C.M.: The drought of the century in the Amazon basin: An
7 analysis of the regional variation of rainfall in South America in 1926, *Acta Amazonica*,
8 35 (2), 231-238, 2005.

9
10 Yoon, J.-H., and Zeng, N.: An Atlantic influence on Amazon rainfall, *Clim. Dyn.*, 34,
11 249-264, doi:10.1007/s00382-009-0551-6, 2010.

12
13 Yu, L., Jin, X., and Weller, R. A.: Multidecade Global Flux Datasets from the
14 Objectively Analyzed Air-sea Fluxes (OAFlux) Project: Latent and sensible heat fluxes,
15 ocean evaporation, and related surface meteorological variables. Woods Hole
16 Oceanographic Institution, OAFlux Project Technical Report. OA-2008-01, 64pp.
17 Woods Hole. Massachusetts, 2008.

	the NA x		the SA x		LP x	
	ONI	AMM	ONI	AMM	ONI	AMM
Jun	0.36 *	-0.02	0.32 *	0.05	0.05	0.13
Jul	0.47 *	0.13	0.37 *	0.07	0.27	0.21
Aug	0.55 *	0.11	0.24	0.10	-0.11	-0.19
Sep	0.31 *	0.03	-0.41 *	-0.02	-0.10	-0.01
Oct	0.33 *	-0.05	-0.16	0.11	0.69 *	0.16
Nov	0.24	0.10	-0.01	-0.22	0.48 *	0.19
Dec	0.26	-0.22	0.04	0.08	0.47 *	-0.20
Jan	0.09	-0.26	-0.34 *	0.27	0.04	0.24
Feb	-0.19	-0.41 *	-0.03	0.38 *	0.03	-0.02
Mar	-0.37 *	-0.31 *	0.34 *	0.41 *	0.18	-0.06
Apr	-0.53 *	-0.69 *	0.50 *	0.62 *	0.48 *	0.31 *
May	-0.38 *	-0.76 *	0.46 *	0.59 *	0.51 *	0.30 *

Table 1: Correlation coefficients between the monthly time series of ONI (and AMM) and: of 10-day (*E-P*) backward trajectories from the Amazon basin integrated over the NA and the SA source regions; of absolute values of 10-day (*E-P*) forward trajectories from the Amazon basin integrated over the LP sink area. All time series cover a 33-year period. Values statistically significant at the 90% level according to a T-Test are denoted *.

Figures Captions:

Figure 1: (left-hand column) Climatological monthly 10-day integrated (*E-P*) values observed for the period June 1979 – May 2012, for all the particles bound for the Amazon basin, determined from backward tracking. Reddish (blueish) colours represent regions acting as moisture sources (sinks) for the tracked particles. Black contour line indicates the basin area. (right-hand column) Climatological monthly vertically integrated moisture flux values (vectors; measured in kg/m/s) and its respective divergence (shade; measured in mm/day). Data obtained from ERA-Interim.

Figure 2a: Climatological annual average of 10-day integrated (E-P) obtained through the backward Amazon experiment for the period June 1979 – May 2012. Black contour line indicates the basin area, and the boxes NA and TA indicate the source areas selected. b: The annual cycle of the monthly values of 10-day (E-P) shown in Fig.1 and integrated over the NA (continuous line) and SA (traced line) source areas indicated in a). Black lines represent the 33-year average values, while pink and green lines indicate the average of the El Niño and La Niña events , respectively. c: as b), but the pink and green lines indicate the average of the AMM+ and AMM- events, respectively.

Figure 3: Climatological monthly 10-day integrated (E-P) fields obtained through the forward Amazon experiment for the period June 1979 – May 2012. Only negative values are shown in order to emphasise the sink regions. Black contour line indicates the basin area.

Figure 4a: Climatological annual average of 10-day integrated (E-P) obtained through the forward Amazon experiment for the period June 1979 – May 2012. Black contour line indicates the basin area, and the LP box indicates the sink area selected. b: The annual cycle of the monthly absolute values of 10-day (E-P) shown in Fig. 3 and integrated over the LP sink area indicated in a). Black lines represent the 33-year average values, while pink and green lines indicate the average of the El Niño and La Niña, respectively. c: as b), but the pink and green lines indicate the average of the AMM+ and AMM- events, respectively.

Figure 5: (left-hand column) Monthly differences of composites of moisture sources of the Amazon basin (considering only positive E-P values in the composites using

backward analysis) for extreme ENSO episodes. Black contour lines indicate regions where the differences are significant at the 90% level according to the bootstrap test. Pink (green) colours indicate regions where the sources are more intense during El Niño (La Niña) years. Blue contour line indicates the basin area. (right-hand column) Monthly differences in the vertically integrated moisture flux (vectors; measured in kg/m/s) and its divergence (shade; measured in mm/day) between the composites for flood and drought years. Data obtained from ERA-Interim.

Figure 6: Differences of composites of moisture sinks of the Amazon basin (considering only negative E-P values in the composites using forward analysis) of extreme ENSO episodes. Black contour lines indicate regions where the differences are significant at the 90% level according to the bootstrap test. Pink (green) colours indicate regions where the sinks are more intense during El Niño (La Niña) years. Blue contour line indicates the basin area.

Figure 7: As Fig 5, but for extreme AMM episodes. Pink (green) colours in the left-hand column indicate regions where the sources are more intense during AMM+ (AMM-) events.

Figure 8: As Fig 6, but for extreme AMM episodes. Pink (green) colours in the left-hand column indicate regions where the sinks are more intense during AMM+ (AMM-) events.

Climatological Conditions (June 1979 - May 2012)

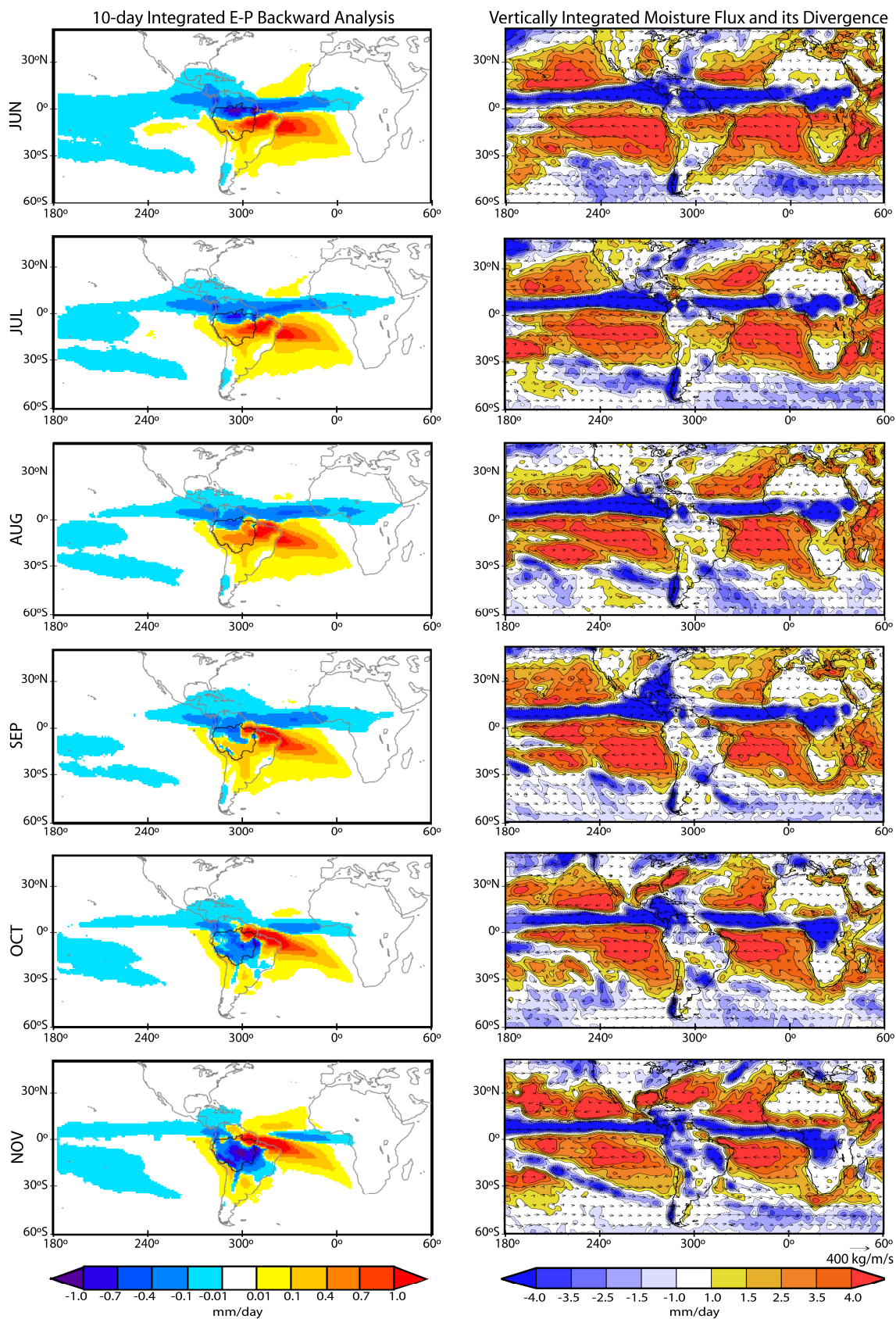


Figure 1

Climatological Conditions (June 1979 - May 2012)

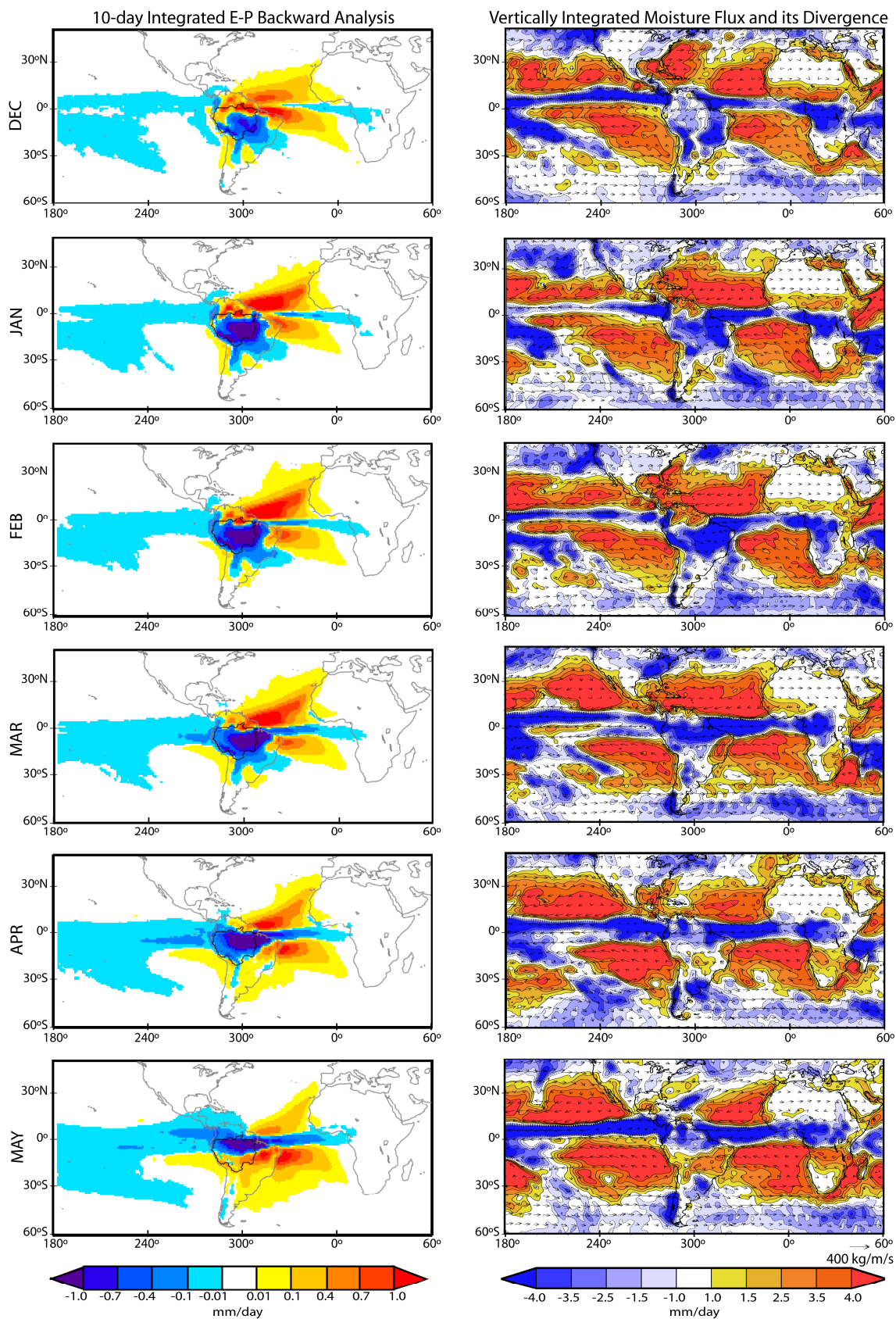


Figure 1 - continuation

Moisture Contribution from the NA and SA regions to the Amazon Basin

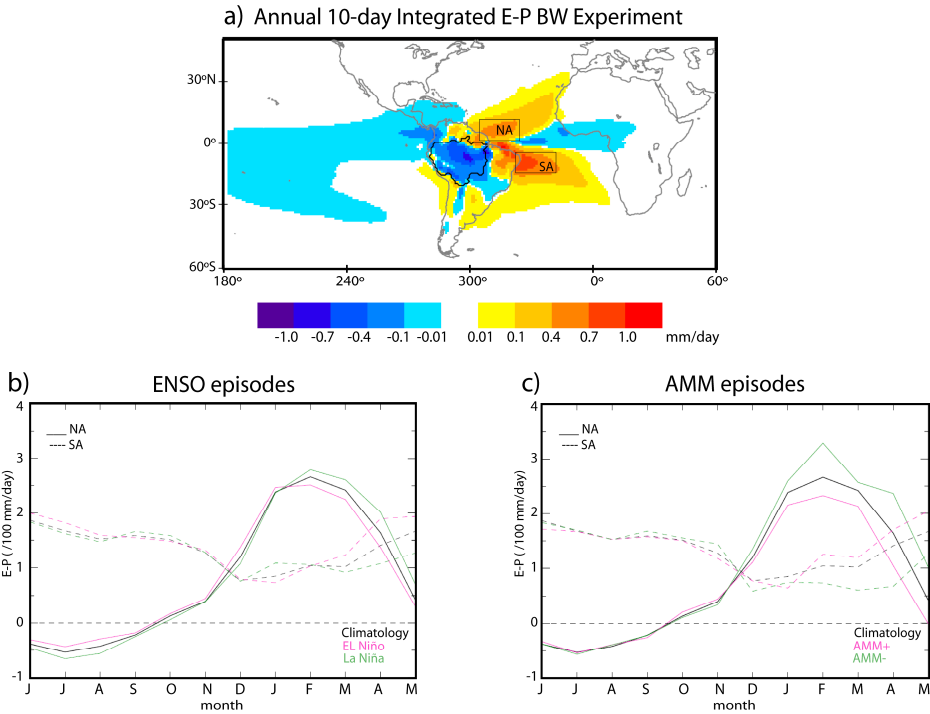


Figure 2

10-day Integrated E-P Forward Analysis - Climatological Conditions

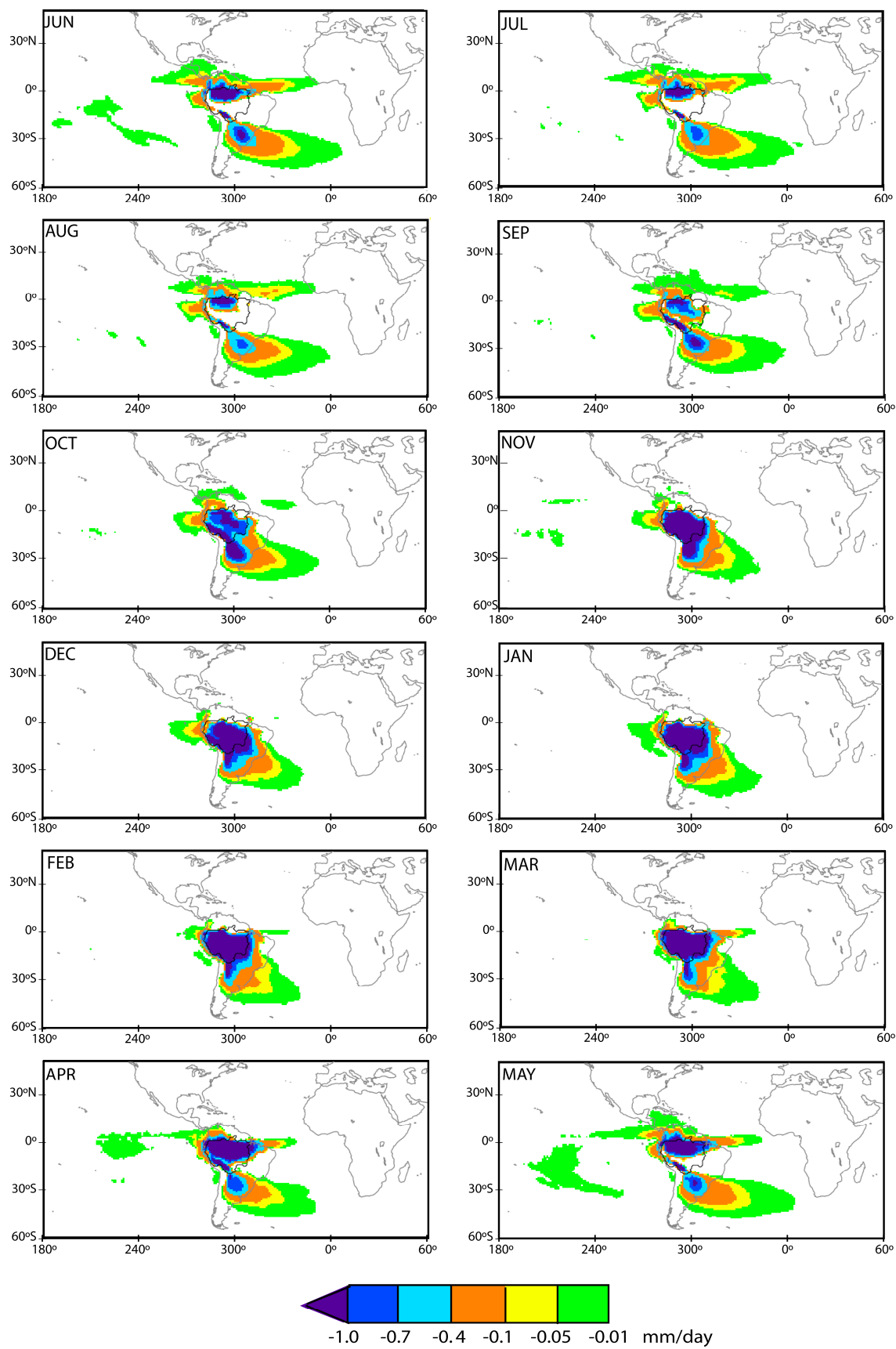


Figure 3

1

Moisture Contribution from the Amazon Basin towards the LP region

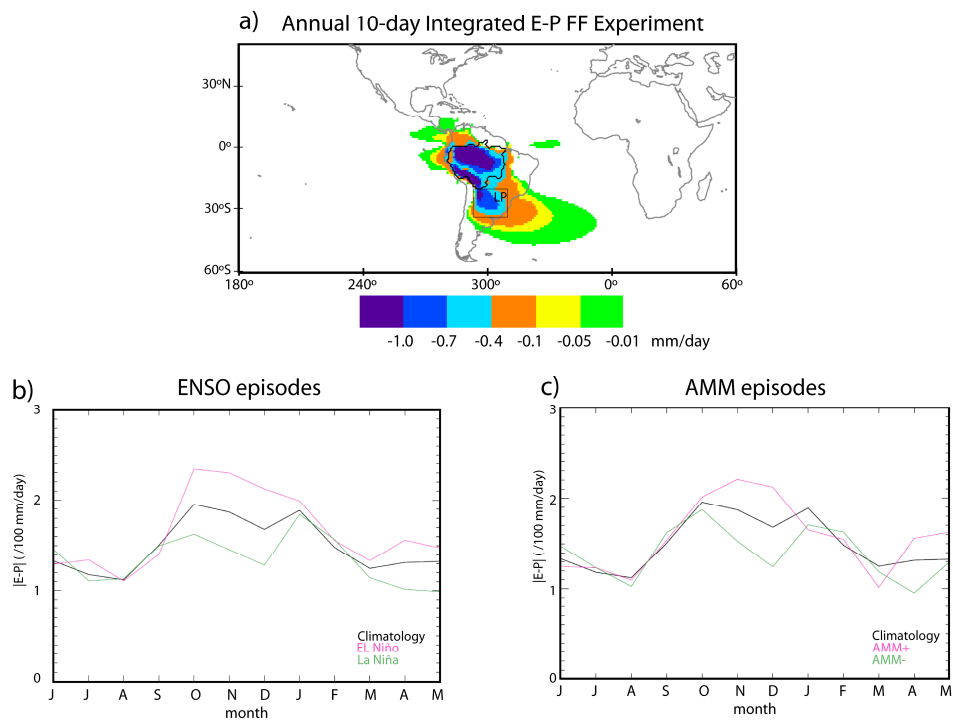


Figure 4

Figure 1 consists of two columns of maps. The left column, titled 'Moisture Source Regions (from Backward Analysis)', shows five maps for the months of June, July, August, September, and October. The right column, titled 'Vertically Integrated Moisture Flux and its Divergence', shows five corresponding maps for the same months. Both columns cover the region from 60°S to 30°N and 180° to 60°E. The maps in the left column use a color scale from -0.5 to 0.5 mm/day, with pink representing negative values and green representing positive values. The maps in the right column use a color scale from -2.5 to 2.5 mm/day, with blue representing negative values and yellow/red representing positive values. Arrows on the right column maps indicate the direction of moisture flux. A color bar at the bottom of each column provides the scale for the moisture flux values.

1

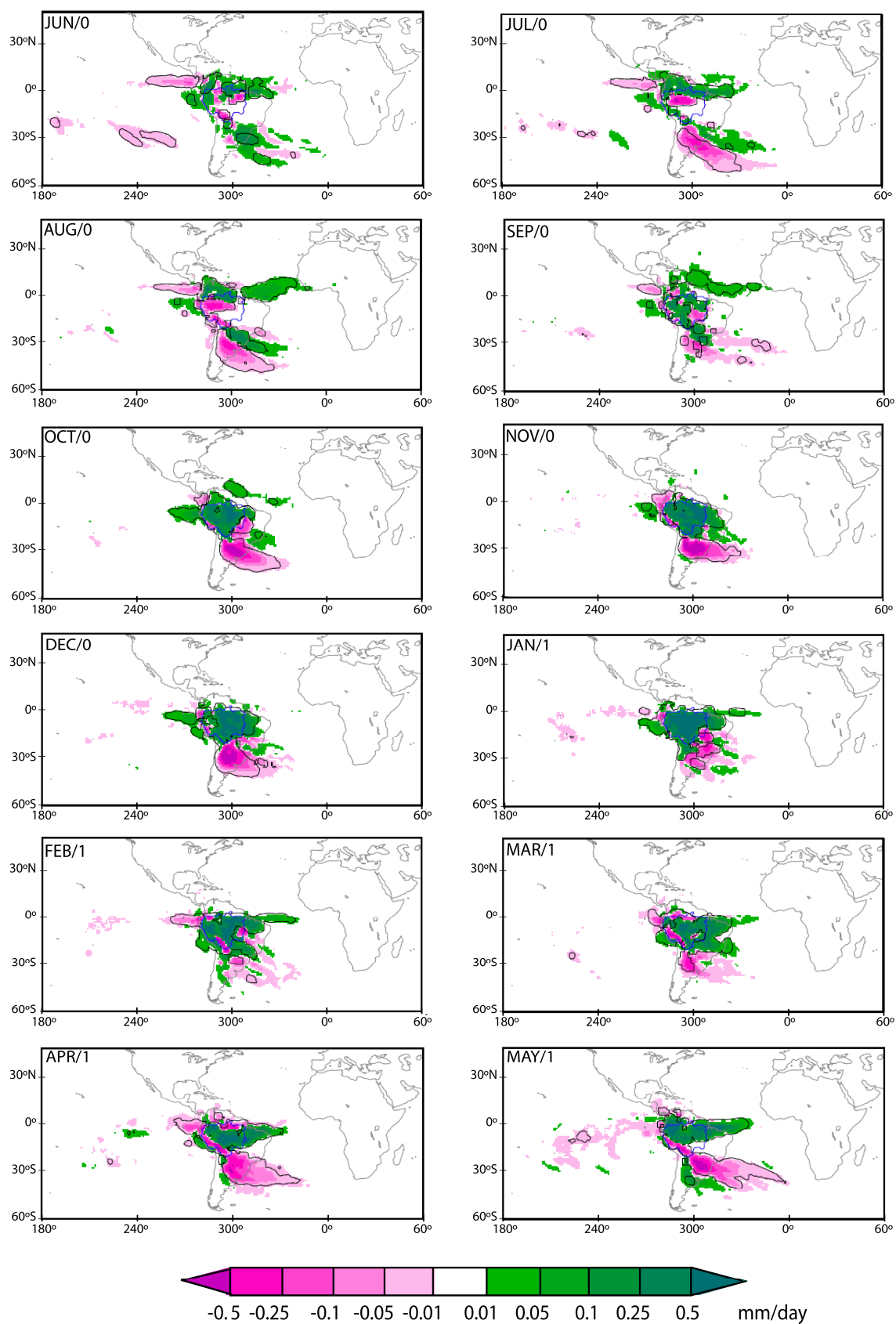
52

Figure 10 consists of two columns of maps. The left column, titled 'Moisture Source Regions (from Backward Analysis)', shows five maps for the months DEC/0, JAN/1, FEB/1, MAR/1, and MAY/1. Each map displays the Amazon basin and surrounding regions, with green and pink shaded areas indicating moisture source regions. The right column, titled 'Vertically Integrated Moisture Flux and its Divergence', shows five corresponding maps for the same months. These maps use color contours and vector arrows to represent moisture flux and divergence. A color bar at the bottom of each column indicates the magnitude of the flux and divergence in mm/day, ranging from -0.5 to 0.5 for the left column and -2.5 to 2.5 for the right column. The maps are labeled with latitude (30°N, 0°, 30°S, 60°S) and longitude (180°, 240°, 300°, 0°, 60°).

1

2

Differences in the Composites of Moisture Sink Regions (from FF Analysis): El Niño - La Niña Years



Differences in the Composites: (AMM+) - (AMM-) Years

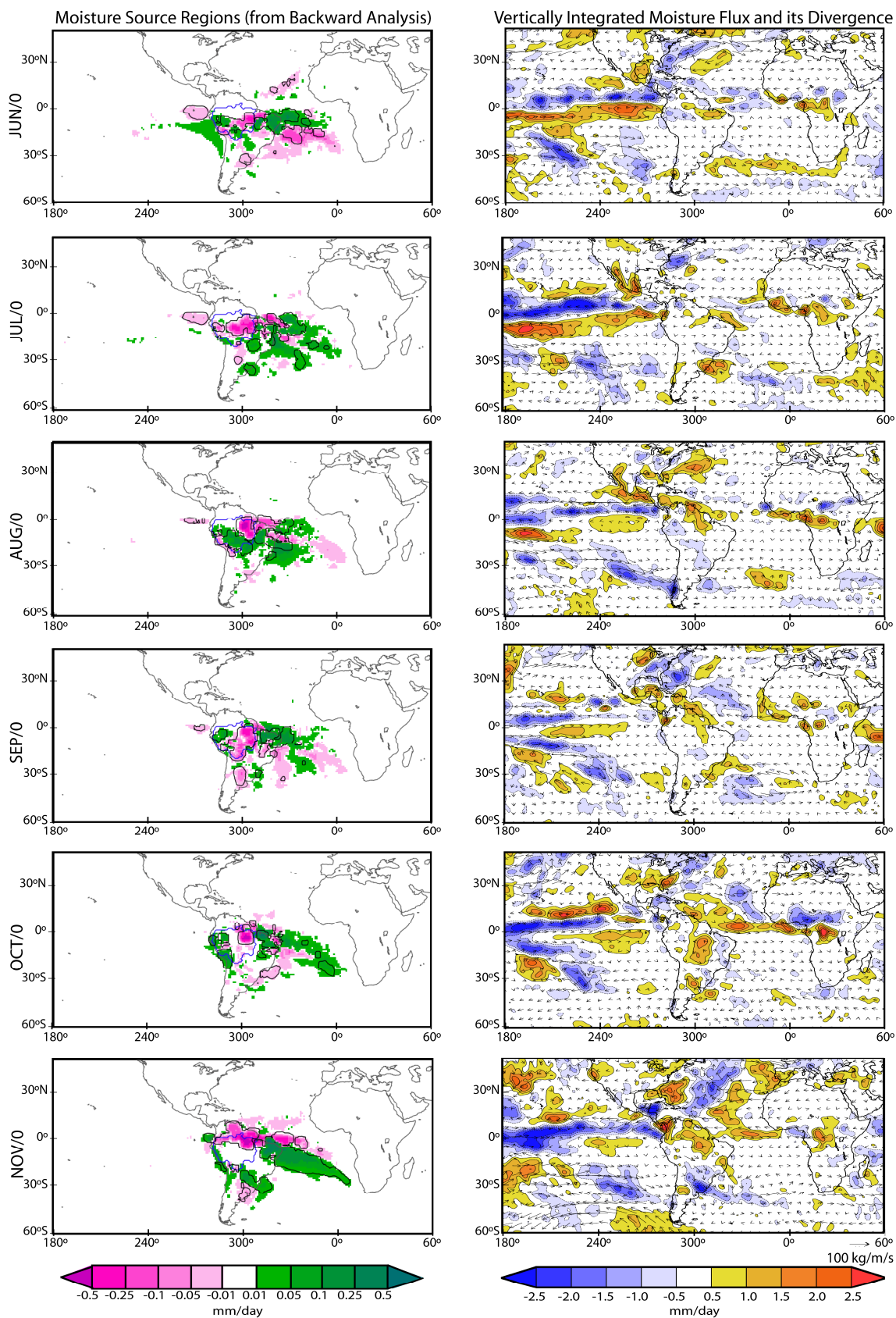


Figure 7

Figure 10 consists of two columns of maps. The left column, titled 'Moisture Source Regions (from Backward Analysis)', shows five maps for the months of December, January, February, March, and April. The right column, titled 'Vertically Integrated Moisture Flux and its Divergence', shows five corresponding maps for the same months. Both columns use a map projection from 180° to 60°E and 60°S to 30°N. The left column maps use a color scale from -0.5 to 0.5 mm/day, with green indicating positive values and pink indicating negative values. The right column maps use a color scale from -2.5 to 2.5 mm/day, with blue indicating negative values and yellow/red indicating positive values. A reference vector for 100 kg/m/s is shown at the bottom right.

Figure 7 – Continuation

56

Differences in the Composites of Moisture Sink Regions (from FF Analysis): (AMM +) - (AMM-) years

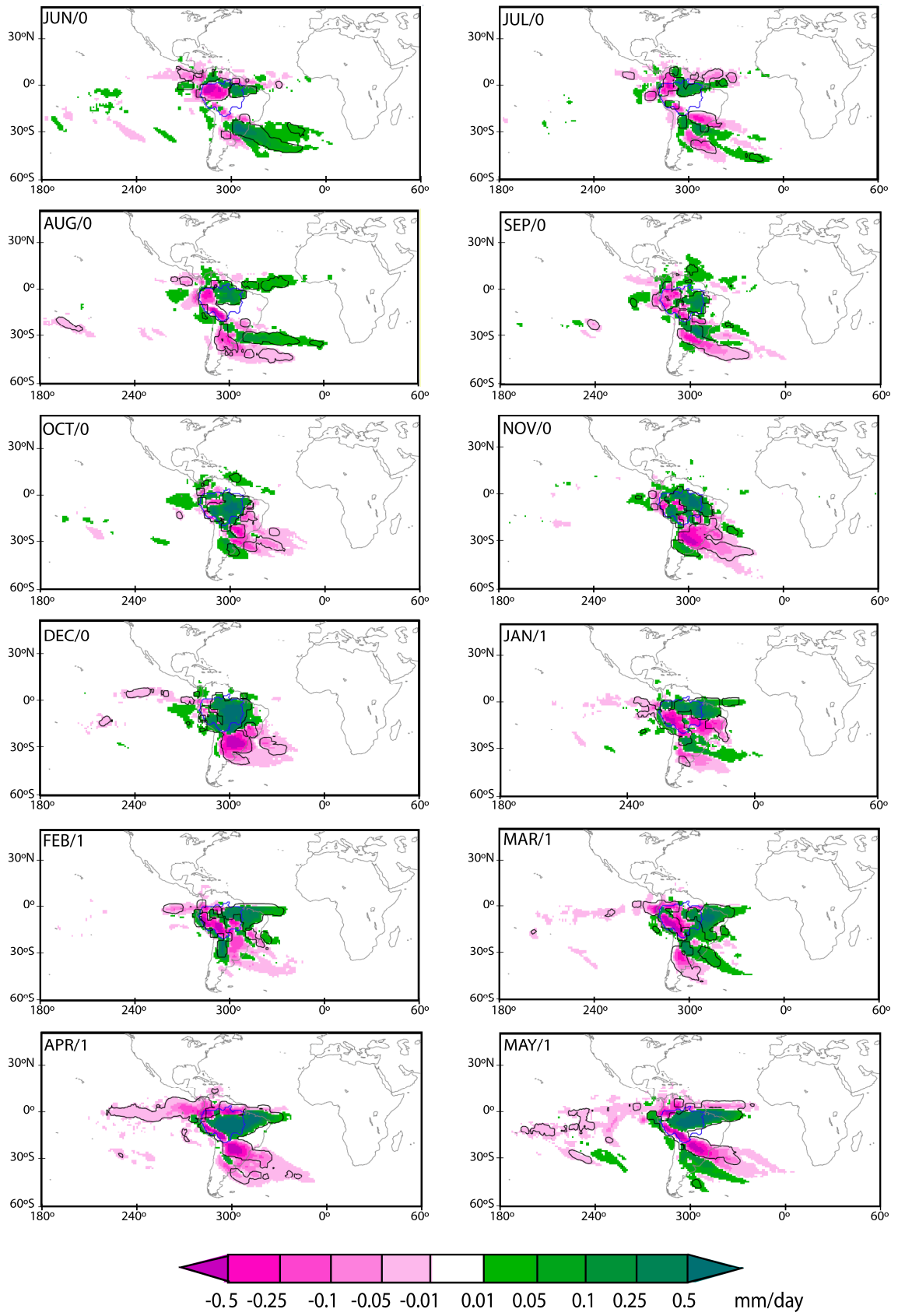


Figure 8